



Received: 20 March 2018
Accepted: 07 May 2018
First Published: 22 May 2018

*Corresponding author: Chayadit Pumaneratkul, Energy Conversion Research Center, Department of Mechanical Engineering, Doshisha University, 1-3 Tatara Miyakodani, Kyotanabe, Kyoto Prefecture 610-0321, Japan
E-mail: eup3502@mail4.doshisha.ac.jp

Reviewing Editor:
Duc Pham, University of Birmingham, UK

Additional information is available at the end of the article

MECHANICAL ENGINEERING | RESEARCH ARTICLE

Exergy analysis of development on supercritical CO₂ solar Rankine cycle system with thermally driven pump

Chayadit Pumaneratkul^{1*}, Takashi Horino¹, Haruhiko Yamasaki² and Hiroshi Yamaguchi¹

Abstract: The innovative development of a thermally driven pump in the supercritical CO₂ solar Rankine cycle system has been carried out and investigated to increase the system efficiency in field operation. To confirm the advantage of the thermally driven pump over conventional mechanical feed pump, the energy and exergy analysis of the system is investigated and discussed. It can be confirmed from the analysis that the thermally driven pump operating under an actual climate condition gives the higher exergetic efficiency in output power to the system compared with the mechanical feed pump. On the contrary, the high rate of exergy destruction is found in the evacuated solar collector under both system conditions. To increase the exergetic efficiency and to prevent the destruction rate, the proper components design, which can be considered as the essential factor to develop the higher performance system, are suggested in the present study.

Subjects: Mechanical Engineering; Renewable Energy; Renewable Energy

Keywords: carbon dioxide; exergy analysis; solar energy; Rankine cycle; thermally driven pump

1. Introduction

Fossil fuels, such as the coal, oil, or gas, which are the leading cause of environmental problems, have been consumed as the power generation sources for many decades. The burning of fossil

ABOUT THE AUTHOR

The authors' research expertise is on the Supercritical CO₂ Flow and Solar Energy Conversion. The focus is to develop the new combined power/heat thermal-fluid cycle with operating temperature range around 30–200°C using CO₂ as a working fluid and utilize solar energy as the energy source, so-called supercritical CO₂ solar Rankine cycle system. The corresponding author, Chayadit Pumaneratkul, is a Ph.D. student at Department of Mechanical Engineering, Doshisha University, Japan. He obtained his B.Eng. in Mechanical Engineering from Kasetsart University, Thailand in 2013 and M.Sc. in Mechanical Engineering from Doshisha University, Japan in 2015.

PUBLIC INTEREST STATEMENT

In the viewpoint of preventing global warming and greenhouse effect, the interest to use CO₂ as a natural working fluid has been given much attention for decades. The utilization of CO₂ in green/renewable energy cycle has been researched and developed. In this study, the energy analysis and exergy analysis of supercritical CO₂ solar Rankine cycle system by using either conventional mechanical feed pump or the thermally driven pump are investigated in a realistic operating condition (field test), and the results are verified to confirm the advantage and superior property of the thermally driven pump against the mechanical feed pump, in which exergy analysis is based on the combination of the first and the second laws of thermodynamics, also able to verify the losses of quality, or work potential in the system.

fuels releases pollutants, such as carbon dioxide (CO₂), sulfur dioxide (SO₂), nitrogen oxide (NO_x), and particulate matter (PM), to the air, which directly affect human health in more significant extent and are considered as the root of global warming and climate change crisis (Hu, Naito, Kobayashi, & Hasatani, 2000). On the other hand, due to the limitation of fossil fuel resources, the world will be led to face the severe energy crisis in the next few decades. Owing to environment and energy issues, utilization of green energy resources is increasingly considered with close attention to promoting in an actual industrial application.

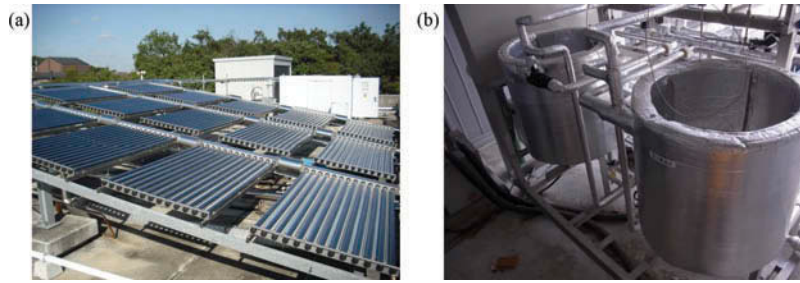
Since 2015, the natural working fluids such as ammonia (NH₃) and carbon dioxide (CO₂) have been recommended to use and utilize as a working fluid in industrial in order to achieve the goal of reducing the carbon emission and to respond the global climate change threat following the “Paris Agreement” (Dimitrov, 2016). In clearing the target of Paris Agreement, the interest in CO₂ as a working fluid in the thermodynamic cycle has increased enormously by taking account of the reasons that CO₂ itself is environmentally friendly compared with other natural working fluids. The flavor comes from the fact that the Ozone Layer Depletion (ODP) and Global Warming Potential (GWP) of CO₂ are defined by 0 and 1, respectively. Moreover, CO₂ can be classified as non-flammable, non-toxic, chemically inactive, and inexpensive in using as a working fluid. Furthermore, CO₂ has high vapor pressure and sizeable volumetric refrigeration capacity, 22,545 kJ/m² at 0°C that the system volume and the changing mass of working fluid are much useful when using CO₂ in the thermodynamic cycle.

Many kinds of research on the utilization of CO₂ in green technology application has been conducted in various aspect of industrial applications, and among which some of the CO₂ application in energy conversion has been much focused in the supercritical state due to the high operation efficiency in a thermodynamic cycle. CO₂ easily becomes to the supercritical state in moderate operation condition due to its low critical point, 7.38 MPa and 31.1°C, respectively, for critical pressure and critical temperature. Given preventing global warming and sustainable energy development, the new supercritical CO₂ thermodynamic cycle with solar input energy for both electric power generation and thermal energy supplies, namely supercritical CO₂ solar Rankine cycle system (SRCS) has been purposed by Zhang, Yamaguchi, Fujima, Enomoto, and Sawada (2005).

The SRCS consists of an evacuated solar collector, turbine, heat exchanger units, and the mechanical feed pump, with which in the previous investigation the fundamental system performance was investigated for the electric and thermal energy generation (Zhang, Yamaguchi, & Uneno, 2007). However, in SRCS, the mechanical feed pump was used as a driving device that the external energy input is required to operate with the mechanical movement part, causing the mechanical loss. From these reasons, the mechanical feed pump resulted in decreasing the overall efficiency of the system with extra consumption from the electric energy generation of SRCS, which reduced the reliability and stability of the system at the same time. To conquer these problems, the new development in SRCS is attempted to develop a thermally driven pump, which was introduced and installed in the system instead of the mechanical feed pump (Kuwahara, Niu, Yamaguchi, Iwamoto, & Zhang, 2011). The outlook of SRCS and thermally driven pump are respectively shown in Figure 1(a) and (b). The thermally driven pump is believed to give advantages of low-quality energy consumption and high reliability to the system. However, in the recent development, the non-continuous flow phenomenon is observed in CO₂ outlet of the thermally driven pump in a trial run due to its intermittent heating and cooling processes.

In this paper, the energy and exergy analysis of SRCS by using either conventional mechanical feed pump or the thermally driven pump are investigated in a realistic operating condition (field test), which the exergy analysis is used to improve the efficiency of the system by energy-resource use (Kanoglu, Dincer, & Rosen, 2007). Moreover, exergy analysis points the specific weakness of the system to design higher efficient system by reducing inefficiencies. For these reasons, the exergy analysis gives the meaningful over energy analysis in term of efficiency evaluation (Hepbasli, 2008; Pope,

Figure 1. Outlook of (a) super-critical CO₂ solar Rankine cycle system and (b) thermally driven pump

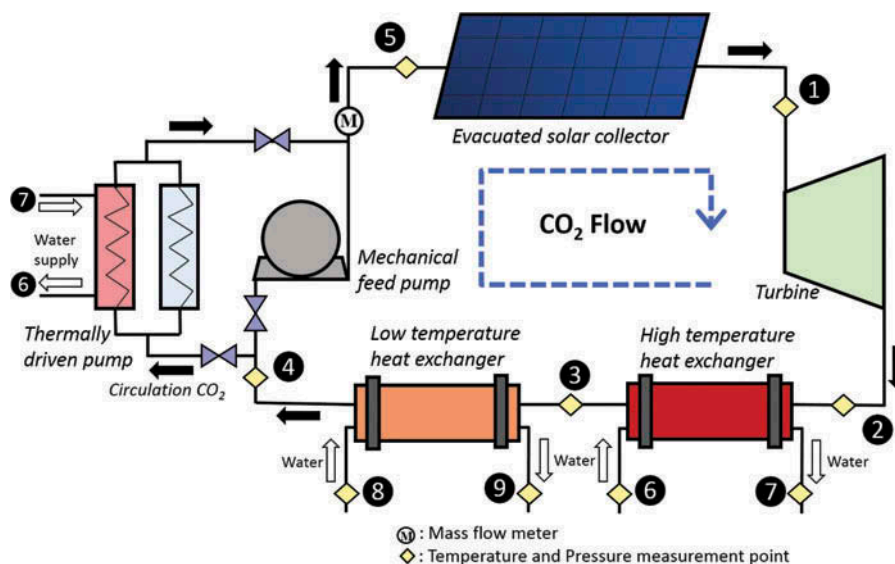


Dincer, & Naterer, 2010). From the analysis results, it is verified to confirm the advantage and superior characteristic of the thermally driven pump against the mechanical feed pump. The details of SRCS with the thermally driven pump will be discussed in next session together with the test conditional (in comparison with the mechanical feed pump).

2. System description

The schematic diagram of SRCS with the mechanical feed pump and with the thermally driven pump is outlined in Figure 2. The SRCS can be operated, and its performance can be examined by using either the mechanical feed pump or the thermally driven pump. As shown in Figure 2, high-pressure CO₂ is heated in evacuated solar collector by solar energy, and it reaches the high-temperature supercritical state (⑤ → ①). At the outlet of the evacuated solar collector, supercritical CO₂ expands and drives the turbine generator. Electric energy is available and obtained from the turbine generator, while the CO₂ becomes a low-pressure state (① → ②). Because of the remaining high-temperature state, the circulation CO₂ is cooled in the high-temperature heat exchanger, with which heat energy can be recovered to use as a heat source for the refrigeration cycle (② → ③). In case of using the thermally driven pump in SRCS, heat energy obtained from the high-temperature heat exchanger is utilized as a heat source for the heating process in the thermally driven pump operation. The low-temperature heat exchanger is used to further cool down CO₂ to the liquid state, while the waste heat energy can be recycled for hot water supply purpose (③ → ④). After leaving heat exchanger units, CO₂ is pumped to the high-pressure state into the evacuated solar collector by the mechanical feed pump or by the thermally driven pump

Figure 2. Schematic diagram of SRCS with the mechanical feed pump and with the thermally driven pump



pump (④ → ⑤), and the cycle recommences. The SRCS is categorized as a trans-critical cycle involving to supercritical point and supercritical region CO₂ inside the Rankine cycle.

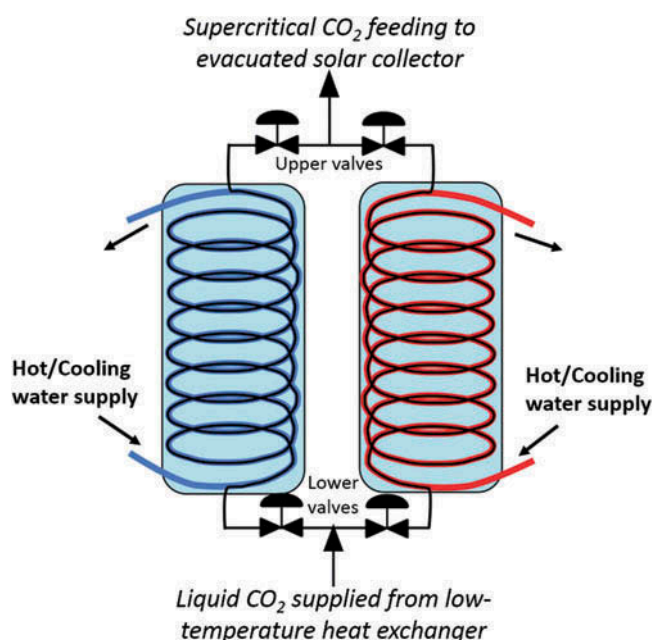
2.1. Novel development: thermally driven pump

The thermally driven pump is a refrigerant (liquid CO₂)-circulation pump, which uses hot and cold water for pressurizing and depressurizing CO₂ inside the device. The thermally driven pump consists of two expansion tanks with cooling and heating function. The schematic of the thermally driven pump is drawn in Figure 3. The expansion tanks are designed and manufactured as a high-pressure vessel with a maximum operating pressure of 12 MPa. In the operation of the thermally driven pump, lower valves are opened, and low-pressure CO₂ (5 MPa) from low-temperature heat exchanger flows into one (lower-pressure tank, while another tank is kept at higher pressure) tank by the exerted pressure difference. After filling CO₂ in one tank, hot water is supplied subsequently for heating CO₂ to high-pressure supercritical state (5–8 MPa), and CO₂ turns into a supercritical state. When CO₂ becomes a high-pressure state in the tank, the upper valve is opened, and the supercritical CO₂ expands and flows toward the evacuated solar collector by the exerted pressure difference. After CO₂ flowing out from the tank, cold water is used to reduce the pressure in the tank (to be lower than 5 MPa), and then the tank is filled by liquid CO₂ from the low-temperature heat exchanger. Following the process, both tanks are continuously operated to achieve progressively high-pressure state and low-pressure state in both tanks, making a thermally driven pump able to charge CO₂ into the evacuated solar collector as if the mechanical feed pump does.

3. Experimental

For the field experiment to investigate the exergy and energy analysis of SRCS, the typical sunny days of the winter season (12 December 2017 and 4 January 2018 for the mechanical feed pump and the thermally driven pump, respectively) at noon in Kyoto, Japan (34°47'58.1"N 135°46'04.6"E), are selected as a reference for measurement. The Correction in experimental method, series arrangement of the evacuated solar collector in 15 panels with the total solar collective area of 9.6 m² (A) is used for the experiment. The factor of wind speed, humidity, and ambient air temperature would also be affected by the CO₂ properties in the system (Chaichan & Kazem, 2016). The T-type thermocouples and pressure sensors with an accuracy of ±0.1°C and ±0.2% for temperature and pressure

Figure 3. Schematic of the thermally driven pump using in SRCS



measurement, respectively, are used to measure temperature and pressure by components in the SRCS while operated (refer to Figure 2). Also, the flow meter is installed at the upstream of the evacuated solar collector with an accuracy of $\pm 0.1\%$. The needle valve as an expander is used in the experiment, instead of an actual turbine, to prevent mechanical loss and to clarify the characteristic of the thermally driven pump alone in the system. The valve is operated in the ambient weather with an adjustable range of 0.0 to 30.00 mm. In the present study, actual electric energy from the turbine generator is not generated from the system as stated above. Therefore, the system performance is estimated based on thermodynamic cycle analysis.

3.1. Thermodynamic cycle analysis of SRCS

The system analysis as described above in a field test is based on a steady state, namely steady flow process, for which mass, energy, and exergy balance equations are adopted by neglecting effects of potential and kinetic energy. The reference state of CO_2 is set for 0°C at saturated liquid, in which enthalpy and entropy set to 200 kJ/Kg and 1.0 kJ/kg-K, respectively, and the reference state of water is adjusted to set as 0 of enthalpy and entropy for 0°C saturated liquid. The efficiencies for the turbine (η_t) and mechanical feed pump (η_{fp}) are respectively assumed as 0.9 and 0.8 for analysis in this study (Zhang et al., 2006). The energy and exergy analysis for SRCS with the mechanical feed pump and with the thermally driven pump are subsequently evaluated and compared in the same operating condition. In the thermally driven pump operation, the energy use in the cooling process is omitted in this study. The flow rate of water in the high-temperature heat exchanger (\dot{m}_{HX1}) and the low-temperature heat exchanger (\dot{m}_{HX2}) are fixed to the range of 600–700 kg/h and 1,200–1,300 kg/h, respectively.

It is noted that all CO_2 thermo-physical properties used in this study are obtained and calculated from PROPATH database (1997), while the properties of water are based on IAPWS by Wagner and Pruß (2002).

4. Evaluation

The thermodynamic cycle performance on energy analysis following the first law of thermodynamics and exergy analysis following the second law of thermodynamics in SRCS are obtained from a mathematical model in components (Grosu, Marin, Dobrovicescu, & Queiros-Conde, 2016; Suzuki, 1988; Tsatsaronis & Cziesla, 2004). The procedure of calculating with the parameters of components, (i) ~ (vi), can be written as follows, by referring Figure 2.

4.1. Evacuated solar collector (process 5–1)

Heat transfer rate \dot{Q}_s of CO_2 in the evacuated solar collector is:

$$\dot{Q}_s = \dot{m}_{\text{CO}_2}(h_1 - h_5) \quad (1)$$

Moreover, the heat loss $\dot{Q}_{\text{loss},s}$ can be estimated as:

$$\dot{Q}_{\text{loss},s} = IA - \dot{Q}_s \quad (2)$$

Thus, the exergy rate that can be calculated from (Petela, 2003):

$$\dot{E}_{\dot{Q}_s} = \dot{Q}_s \left[1 + \frac{1}{3} \left(\frac{T_0}{T_{sr}} \right)^4 - \frac{4}{3} \left(\frac{T_0}{T_{sr}} \right) \right] \quad (3)$$

where T_0 is the ambient temperature, and T_{sr} is the solar radiation temperature assumed as 5,800 K (Ruppel & Wurfel, 1980).

The change in exergy rate $\dot{E}_1 - \dot{E}_5$ across the evacuated solar collector can be determined as:

$$\dot{E}_1 - \dot{E}_5 = \dot{m}_{\text{CO}_2}[h_1 - h_5 - T_0(s_1 - s_5)] \quad (4)$$

Finally, the exergy destruction rate Π_s should be obtained as:

$$\Pi_s = \dot{E}_{\dot{Q}_s} - (\dot{E}_1 - \dot{E}_5) \quad (5)$$

4.2. Turbine (process 1–2)

Energy balance \dot{Q}_t in turbine (the expansion valve) is:

$$\dot{Q}_t = \dot{m}_{\text{CO}_2}(h_1 - h_2) \quad (6)$$

The power W_t of the turbine can be written as:

$$W_t = \dot{Q}_t \eta_t \quad (7)$$

Moreover, the exergy rate change $\dot{E}_1 - \dot{E}_2$ from the inlet and outlet of the turbine is:

$$\dot{E}_1 - \dot{E}_2 = \dot{m}_{\text{CO}_2}[h_1 - h_2 - T_0(s_1 - s_2)] \quad (8)$$

Thus, the exergy destruction rate Π_t of the turbine is calculated as:

$$\Pi_t = (\dot{E}_1 - \dot{E}_2) - W_t \quad (9)$$

4.3. High-temperature heat exchanger (process 2–3)

The heat transfer rate \dot{Q}_{HX1} leaving high-temperature heat exchanger is:

$$\dot{Q}_{\text{HX1}} = \dot{m}_{\text{Water}_{\text{HX1}}}(h_7 - h_6) \quad (10)$$

For heat loss $\dot{Q}_{\text{loss,HX1}}$ in the high-temperature heat exchanger, it can be calculated as:

$$\dot{Q}_{\text{loss,HX1}} = \dot{m}_{\text{CO}_2}(h_2 - h_3) - \dot{m}_{\text{Water}_{\text{HX1}}}(h_7 - h_6) \quad (11)$$

The exergy balance $\dot{E}_2 - \dot{E}_3$ across the high-temperature heat exchanger can be written as:

$$\dot{E}_2 - \dot{E}_3 = \dot{m}_{\text{CO}_2}[h_2 - h_3 - T_0(s_2 - s_3)] \quad (12)$$

Furthermore, exergy balance rate $\dot{E}_7 - \dot{E}_6$ for water heat absorption in the high-temperature heat exchanger is determined as:

$$\dot{E}_7 - \dot{E}_6 = \dot{m}_{\text{Water}_{\text{HX1}}}[h_7 - h_6 - T_0(s_7 - s_6)] \quad (13)$$

Thus, the exergy destruction rate Π_{HX1} of the high-temperature heat exchanger can be obtained from:

$$\Pi_{\text{HX1}} = (\dot{E}_2 - \dot{E}_3) - (\dot{E}_7 - \dot{E}_6) \quad (14)$$

4.4. Low-temperature heat exchanger (process 3–4)

The heat transfer rate \dot{Q}_{HX2} leaving low-temperature heat exchanger is calculated as:

$$\dot{Q}_{\text{HX2}} = \dot{m}_{\text{Water}_{\text{HX2}}}(h_9 - h_8) \quad (15)$$

Heat loss $\dot{Q}_{\text{loss,HX2}}$ in low-temperature heat exchanger is:

$$\dot{Q}_{\text{loss,HX2}} = \dot{m}_{\text{CO}_2}(h_3 - h_4) - \dot{m}_{\text{Water}_{\text{HX2}}}(h_9 - h_8) \quad (16)$$

For the exergy balance $\dot{E}_3 - \dot{E}_4$ across the low-temperature heat exchanger, it can be obtained from:

$$\dot{E}_3 - \dot{E}_4 = \dot{m}_{\text{CO}_2}[h_3 - h_4 - T_0(s_3 - s_4)] \quad (17)$$

Moreover, exergy balance rate $\dot{E}_9 - \dot{E}_8$ for water heat absorption in the low-temperature heat exchanger is:

$$\dot{E}_9 - \dot{E}_8 = \dot{m}_{\text{Water}_{\text{HX2}}}[h_9 - h_8 - T_0(s_9 - s_8)] \quad (18)$$

Hence, the exergy destruction rate Π_{HX2} of the low-temperature heat exchanger can be calculated as:

$$\Pi_{HX2} = (\dot{E}_3 - \dot{E}_4) - (\dot{E}_9 - \dot{E}_8) \tag{19}$$

4.5. Mechanical feed pump (process 4–5)

Energy balance \dot{Q}_{fp} of mechanical feed pump is:

$$\dot{Q}_{fp} = \dot{m}_{CO_2}(h_5 - h_4) \tag{20}$$

And the power required W_{fp} for mechanical feed pump can be estimated as:

$$W_{fp} = \frac{\dot{Q}_{fp}}{\eta_{fp}} \tag{21}$$

The change of exergy $\dot{E}_5 - \dot{E}_4$ from state 4 to state 5 is:

$$\dot{E}_5 - \dot{E}_4 = \dot{m}_{CO_2}[h_5 - h_4 - T_0(s_5 - s_4)] \tag{22}$$

Thus, the exergy destruction rate Π_{fp} in mechanical feed pump is obtained from:

$$\Pi_{fp} = W_{fp} - (\dot{E}_5 - \dot{E}_4) \tag{23}$$

4.6. Thermally driven pump (process 4'–5')

Energy balance \dot{Q}_{tp} for the thermally driven pump is:

$$\dot{Q}_{tp} = \dot{m}_{CO_2}(h_5 - h_4) \tag{24}$$

And the change in exergy $\dot{E}_5 - \dot{E}_4$ across thermally driven pump is calculated as:

$$\dot{E}_5 - \dot{E}_4 = \dot{m}_{CO_2}[h_5 - h_4 - T_0(s_5 - s_4)] \tag{25}$$

For the exergy destruction rate Π_{tp} in the thermally driven pump, it can be estimated as:

$$\Pi_{tp} = (\dot{E}_5 - \dot{E}_4) + (\dot{E}_7 - \dot{E}_6) \tag{26}$$

Deriving the performance by components above, (i) ~ (vi), the overall performance of the system will be given for the system thermal efficiency of SRCS with the mechanical feed pump ($\eta_{th,fp}$) and with the thermally driven pump ($\eta_{th,tp}$), respectively, as:

$$\eta_{th,fp} = \frac{W_{net,fp}}{Q_{in}} = \frac{W_t + \dot{Q}_{HX1} + \dot{Q}_{HX2} - W_{fp}}{\dot{Q}_s} \tag{27}$$

and

$$\eta_{th,tp} = \frac{W_{net,tp}}{Q_{in}} = \frac{W_t + \dot{Q}_{HX2}}{\dot{Q}_s} \tag{28}$$

The exergetic efficiency, the evaluation on the actual performance of an energy system from the thermodynamic viewpoint of SRCS with the mechanical feed pump ($\eta_{e,fp}$) and with the thermally driven pump ($\eta_{e,tp}$) can be written as:

$$\eta_{e,fp} = \frac{W_t + (\dot{E}_7 - \dot{E}_6) + (\dot{E}_9 - \dot{E}_8)}{\dot{E}_{\dot{Q}_s} + W_{fp}} \tag{29}$$

and

$$\eta_{e,tp} = \frac{W_t + (\dot{E}_9 - \dot{E}_8)}{\dot{E}_{\dot{Q}_s}} \tag{30}$$

For the exergy destruction, which is a measure of the irreversibility in an object is an essential parameter in exergy modeling, it can be defined here from the potential work lost due to the irreversibility in a specific element of the system. The total exergy destruction of SRCS with the mechanical feed pump ($\Pi_{\text{Total,fp}}$) and with the thermally driven pump ($\Pi_{\text{Total,tp}}$) can be thus defined as:

$$\Pi_{\text{Total,fp}} = \Pi_s + \Pi_t + \Pi_{\text{HX1}} + \Pi_{\text{HX2}} + \Pi_{\text{fp}} \quad (31)$$

and

$$\Pi_{\text{Total,tp}} = \Pi_s + \Pi_t + \Pi_{\text{HX2}} + \Pi_{\text{tp}} \quad (32)$$

By the contribution of components, (i) ~ (vi), the total exergy destruction rate η_{Π_i} in SRCS can be remitted as follows:

$$\eta_{\Pi_i} = \frac{\Pi_i}{\Pi_{\text{Total}}} \quad (33)$$

where Π_i is referred to the exergy destruction rate by components, (i) ~ (vi), in SRCS.

Finally, for by components of SRCS, the exergetic efficiency, which characterizes the performance of a system component from the thermodynamic viewpoint, can be defined by the exergetic availability (Spayde, Mago, & Cho, 2017). The resultant equations for the exergetic efficiency for the evacuated solar collector, turbine, high-temperature heat exchanger, low-temperature heat exchanger, mechanical feed pump, and thermally driven pump can be found below, respectively.

$$\eta_{x,s} = \frac{\dot{E}_1 - \dot{E}_5}{\dot{E}_{Q_s}} \quad (34)$$

$$\eta_{x,t} = \frac{\dot{E}_t}{\dot{E}_1 - \dot{E}_2} = \frac{t}{\dot{E}_1 - \dot{E}_2} \quad (35)$$

$$\eta_{x,\text{HX1}} = \frac{\dot{E}_7 - \dot{E}_6}{\dot{E}_2 - \dot{E}_3} \quad (36)$$

$$\eta_{x,\text{HX2}} = \frac{\dot{E}_9 - \dot{E}_8}{\dot{E}_3 - \dot{E}_4} \quad (37)$$

$$\eta_{x,\text{fp}} = \frac{\dot{E}_5 - \dot{E}_4}{\dot{E}_{\text{fp}}} = \frac{\dot{E}_5 - \dot{E}_4}{W_{\text{fp}}} \quad (38)$$

$$\eta_{x,\text{tp}} = \frac{\dot{E}_{5'} - \dot{E}_{4'}}{\dot{E}_7 - \dot{E}_6} \quad (39)$$

5. Results and discussion

For the calculation on the energy and exergy analysis of SRCS, the operation conditions of CO₂ circulation and hot/cooling water supply in each state are tabulated, where Tables 1 and 2 present the parametric data for the operation of SRCS with the mechanical feed pump and the thermally driven pump, respectively. In the tables, it is noted that temperature, pressure, enthalpy, and mass flow rate of CO₂ circulation and hot/cooling water supply are given according to the thermodynamic process specified in Figure 2.

The *P-h* cycle diagrams of SRCS with the two conditions (Tables 1 and 2) are shown in Figure 4. Approximately the same value of solar radiation on time average during the experiments are selected for the field operation of SRCS for the sake of comparison between the mechanical feed

Table 1. Conditions of SRCS with the mechanical feed pump

State	Fluid	Phase	\dot{m} (kg/s)	P (MPa)	T (°C)	h (kJ/kg)	s (kJ/kg-K)
①	CO ₂	Supercritical	0.0075	8.11	148.98	881.85	4.268
②	CO ₂	Low pressure superheated vapor	0.0075	4.34	101.92	850.08	4.293
③	CO ₂	Low pressure superheated vapor	0.0075	4.37	14.03	738.38	3.952
④	CO ₂	Vapor-liquid mixture	0.0075	4.36	8.72	524.58	3.194
⑤	CO ₂	Compressed liquid	0.0075	8.02	15.10	535.40	3.218
⑥	Water	Liquid	0.19	0.101325	20.88	87.36	0.308
⑦	Water	Liquid	0.19	0.101325	21.62	90.70	0.319
⑧	Water	Liquid	0.36	0.101325	6.33	26.58	0.096
⑨	Water	Liquid	0.36	0.101325	7.23	30.49	0.110

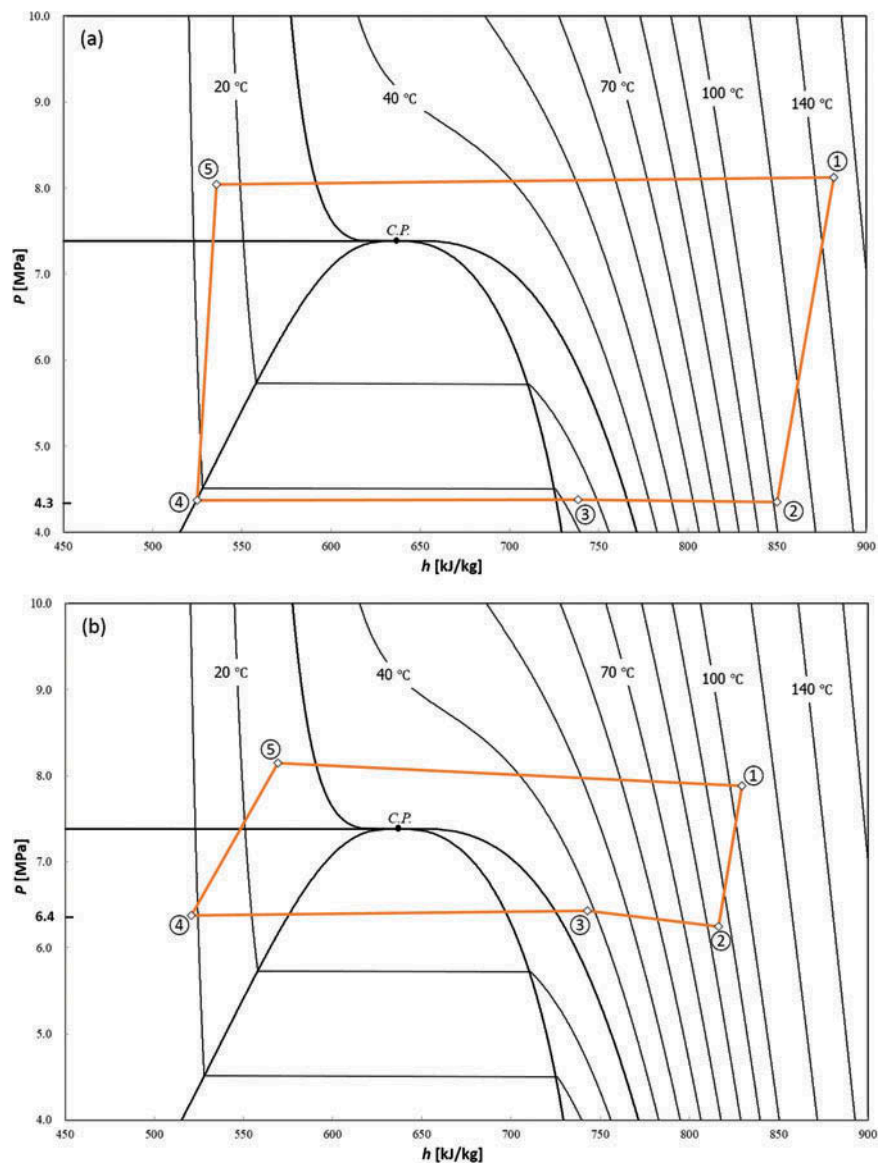
Table 2. Conditions of SRCS with the thermally driven pump

State	Fluid	Phase	\dot{m} (kg/s)	P (MPa)	T (°C)	h (kJ/kg)	s (kJ/kg-K)
①	CO ₂	Supercritical	0.0085	7.89	105.21	829.45	4.141
②	CO ₂	Low pressure superheated vapor	0.0085	6.26	85.02	816.34	4.142
③	CO ₂	Low pressure superheated vapor	0.0085	6.44	38.29	742.84	3.919
④	CO ₂	Low pressure liquid	0.0085	6.39	8.67	520.99	3.173
⑤	CO ₂	Compressed liquid	0.0085	8.15	26.41	569.93	3.333
⑥	Water	Liquid	0.17	0.101325	41.20	172.63	0.588
⑦	Water	Liquid	0.17	0.101325	42.41	177.65	0.604
⑧	Water	Liquid	0.36	0.101325	8.71	36.66	0.131
⑨	Water	Liquid	0.36	0.101325	9.82	41.28	0.148

pump and the thermally driven pump. The time-averaged values are respectively 0.459 kW/m² and 0.422 kW/m². As shown in Figure 4, the transcritical CO₂ thermodynamic cycles are achieved in both SRCS with the mechanical feed pump and with the thermally driven pump throughout the operation. In Figure 4 (a), it can be obviously seen that the cycle reaches to the supercritical high pressure state at around 8 MPa, where the simultaneous heating process takes place at the temperature from 15.1°C to 148.98°C in evacuated solar collector (⑤ → ① in Figure 4(a)). For the subcritical low pressure, the pressure at around 4.3 MPa is obtained with heat recovery process of 101.92–8.72°C in heat exchanger units (② → ④ in Figure 4(a)). Particularly in case of SRCS with the thermally driven pump, the pressure of around 8 MPa and the temperature rise from 26.41°C to 105.21°C is achieved at a supercritical high pressure state in the heating process (evacuated solar collector, ⑤ → ① in Figure 4(b)). For the subcritical low pressure, the pressure of around 6.4 MPa and the temperature from 85.02°C to 8.67°C is obtained in the heat recovery process (heat exchanger units, ② → ④ in Figure 4(b)).

From both cycle conditions, it can be observed that the heating processes in the Rankine cycle are in the supercritical region for CO₂. That is to say, under the supercritical state, CO₂ absorbs the thermal energy (heat energy) in the evacuated solar collector. Also, small pressures

Figure 4. *P-h* diagram of SRCS with (a) the mechanical feed pump and with (b) the thermally driven pump



changes are found between the pump component and evacuated solar collector, and between the heat exchanger units for both cycle conditions. It can be indicated that the flow through these components is continuous (in Figure 4). The pressure difference in the cycle (supercritical high pressure and subcritical low pressure) of SRCS with the mechanical feed pump and with the thermally driven pump is approximately 2.7 MPa and 1.6 MPa, respectively. The lower in pressure difference in the cycle with the thermally driven pump is due to the working principle of the thermally driven pump itself, indicating that the oscillatory flow in the cycle is inevitable throughout the alternative heating and cooling process (Yamaguchi, Zhang, Niu, & Hashitani, 2013). In the operating range of transcritical CO₂ cycle system, it is understood that the pressure difference of the turbine generator affects the system thermal efficiency in more significant extent (Guo, Wang, & Zhang, 2010).

In the energy analysis, the input energy rate of SRCS when the mechanical feed pump is used obtained from Equation (1) together with Equation (20) is 4.508 kW, which comes from the evacuated solar collector and mechanical feed pump, respectively, while the output energy rate of operating SRCS is 2.257 kW, which comes from both the turbine generator, Equation (7), and

heat recovery from heat exchanger units, Equations (10) and (15). For the SRCS with the thermally driven pump, however, the input energy rate is only from the evacuated solar collector, Equation (1), which is 4.032 kW, and the output energy of 1.763 kW comes from both the turbine and low-temperature heat exchanger with Equations (7) and (15), respectively. It can be found that the output energy rate of SRCS with the thermally driven pump is lower than that with the mechanical feed pump. The reason is chiefly that of the output energy from the high-temperature heat exchanger, for which additional energy has to be supplied to the thermally driven pump itself for operation, although there is no actual electric energy consumption is required in operation.

Based on the field operation as shown in Figure 4, the system thermal efficiency of SRCS can be calculated from Equations (27) and (28). It is found that SRCS with the mechanical feed pump gives higher efficiency compared with the thermally driven pump, which is respectively 82.64% and 79.87%. The lower in thermal efficiency is due to the low pressure difference in the cycle of SRCS with the thermally driven pump. Furthermore, the slightly lower solar radiation has also been affected by the thermal efficiency to some extent. It is noted here that there is no electric energy consumption required to operate the thermally driven pump, with which the total electric energy can be generated genuinely from the power device (turbine generator) of the system without any external electric energy consumption.

In term of exergetic efficiency, the rational performance to compare both quantities of input and output energy in the system, which can be obtained from Equations (29) and (30) for SRCS with the mechanical feed pump and with the thermally driven pump, are 11.47% and 20.28%, respectively. The higher in the exergetic efficiency of SRCS with the thermally driven pump is derived from the fact that the thermally driven pump gives much high-quality energy that is available to convert to work compared with the mechanical feed pump. From the efficiencies analysis of the system, it can be speculated that the different values of the efficiency come from the irreversibility in the process by components in the thermal efficiency calculation.

Table 3 shows the contribution (in percentage term) by components in the system to total exergy destruction rate, which is obtained in Equations (31)–(33) for SRCS with the mechanical feed pump or with the thermally driven pump. The exergy destruction represents the exergy destroyed in the irreversibility process by components, which are caused by many factors such as heat transfer loss, friction or chemical reaction (Mago, Srinivasan, Chamra, & Somayaji, 2008). In case of SRCS with the mechanical feed pump, the evacuated solar collector has 89.99% of exergy destruction rate, and the turbine has next highest percent contribution with a value of 3.31%, following the mechanical feed pump, the low-temperature heat exchanger and the high-temperature heat exchanger (3.01%, 2.47%, and 1.23%, respectively). For the SRCS with the thermally driven pump, the exergy destruction rate of 76.28%, 12.63%, and 10.57% are found in the evacuated solar collector, the low-temperature heat exchanger and the thermally driven pump itself, respectively, while the lowest contribution can be found in the turbine at only 0.51%. It is indicated that the thermally driven pump gives better performance characteristic in the term of exergy efficiency in the electric energy generation to the system. From Table 3, it can be observed that the highest contribution to the exergy destruction rate can be found in the evacuated solar collector for both system conditions. It is due to the high rate of heat losses occurred in the evacuated solar collector.

Table 3. Percentage of exergy destruction rate by components							
SRCS	Π_s	Π_t	Π_{HX1}	Π_{HX2}	Π_{fp}	Π_{tp}	%
with mechanical feed pump	89.99	3.31	1.23	2.47	3.01		
with thermally driven pump	76.28	0.51		12.63		10.57	

It is noticed from Table 3 that the thermally driven pump (Π_{tp}) itself has higher order contribution to the total exergy destruction rate in comparison with the mechanical feed pump (Π_{fp}). The reason can be thought that the thermal energy (heat energy) of the thermally driven pump is much higher than that of the electric energy input to the mechanical feed pump when the exergy is calculated.

The calculated exergetic parameters of components are listed in Table 4 for the representative operation (Figure 4) of SRCS with the mechanical feed pump or with the thermally driven pump. Table 4 shows exergetic efficiency (obtained from Equations (34) through (39)) of evacuated solar collector $\eta_{x,s}$, turbine $\eta_{x,t}$, high-temperature heat exchanger $\eta_{x,HX1}$, low-temperature heat exchanger $\eta_{x,HX2}$, and the mechanical feed pump $\eta_{x,fp}$ or the thermally driven pump $\eta_{x,tp}$ for both system conditions. From the presented results, it can be inferred that the turbine has exergetic efficiencies of 72.86% and 88.74% for the operation of representative SRCS with the mechanical feed pump or with the thermally driven pump, respectively. These efficiencies can be considered as relatively high, indicating that the turbine component can be regarded as the highest performance component, in which the electric power generation from the turbine can be considered as a principal (high quality) output energy of SRCS rather than the thermal energy supplied from heat exchanger units. On the other hand, relative low exergetic efficiency is found in the evacuated solar collector component for both mechanical feed pump and thermally driven pump conditions (10.30% and 7.84%, respectively). The heat exchanger units in SRCS with the mechanical feed pump has higher exergetic efficiencies, which are 60.00% and 33.86% for high-temperature heat exchanger and low-temperature heat exchanger, respectively, compared with the thermally driven pump, 23.15%, and 0.92%, respectively. The reasons of low in the exergetic efficiency in heat exchanger units are mainly due to the irreversibility associated with heat transfer over finite temperature differences (Chen et al., 2009). Moreover, the operation characteristic of the thermally driven pump can be considered as the same characteristic as heat exchanger operation (evaporator), which resultantly shows lower in the exergetic efficiency (3.03%).

The exergy destruction rates by components are given in Table 3, while the exergetic efficiencies by components are given in Table 4. Here, it can be observed from the tables that the evacuated solar collector has maximum exergy destruction rate and low exergetic efficiency in both system conditions. To increase the performance and reduce the exergy destruction of SRCS, careful attention should be paid to the heat losses from the evacuated solar collector. The optimum design of the evacuated solar collector must be suggested to be developed for the further efficient system.

Since the thermally driven pump has been developed for the purpose to increase the overall performance of SRCS, weather conditions of summer season and autumn season are acquired to evaluate the exergetic efficiency by components under SRCS operation. The typical days in summer season (29 August) and autumn season (9 November) are selected as references also of the winter season (4 January) for the field test of SRCS with the thermally driven pump. Figure 5 presents the comparison of the exergetic efficiency by components (i.e., evacuated solar collector, turbine, high-temperature heat exchanger, low-temperature heat exchanger, and thermally driven pump) in three weather conditions. It can be found that the exergetic efficiency of the turbine is the highest in the winter season. The reason is from the pressure difference between the supercritical (high) pressure and subcritical (low) pressure in the cycle, that is, a higher (1.6 MPa) in winter as compared with autumn and summer seasons (1.4 MPa and 0.9 MPa, respectively).

The exergetic efficiency of the high-temperature heat exchanger can be found at the highest in summer season (64%), while the lowest efficiency is in the winter season (23.15%), as indicated in

Table 4. Exergetic efficiencies by components

SRCS	$\eta_{x,s}$	$\eta_{x,t}$	$\eta_{x,HX1}$	$\eta_{x,HX2}$	$\eta_{x,fp}$	$\eta_{x,tp}$	%
with mechanical feed pump	10.30	72.86	60.00	33.86	28.24		
with thermally driven pump	7.84	88.74	23.15	0.92		3.03	

Figure 5. Percentage of exergetic efficiencies by components in SRCS with the thermally driven pump in summer season (29 August), autumn season (9 November), and winter season (4 January)

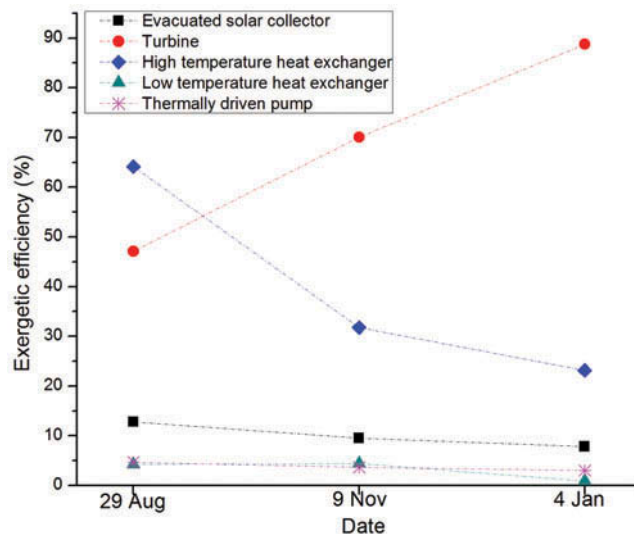


Figure 5. The trend comes from low ambient temperature in winter season effects directly to water temperature used in the heat exchanger. However, the variation of exergetic efficiency in the evacuated solar collector, the low-temperature heat exchanger, and the thermally driven pump shows minimal change in weather conditions as shown in Figure 5.

From the results as obtained in Figure 5, it can be observed that the factor in weather condition has much effect on the exergetic efficiency of the turbine and the high-temperature heat exchanger. Although in the present study, the SRCS field test gave the excellent understanding of the performance characteristic of the system and as well as to the consists of components, further factors (such as wind and humidity) may have to be considered for further obtaining accurate data in the more detailed understanding of the system.

The analysis of exergetic efficiency in SRCS is a methodological approach to investigate the performance of the system. It can help to assess and compare energy conversion system with different weather conditions. The energy analysis conducted in the present study provides a primary inspect of technological efficiencies, whereas the exergy analysis gives detailed understanding to imperfections of the energy conversion systems. The components in SRCS have to be developed with higher efforts to increase the energy and exergy efficiency, also to prevent the losses in term of energy and exergy, especially in the evacuated solar collector. Furthermore, the thermally driven pump, which plays an essential role as a critical development element in the renewable energy cycle system, has to be further investigated for higher overall efficiency.

6. Conclusions

The systematic comparison with the energy and exergy analysis of SRCS with the mechanical feed pump or the thermally driven pump is presented. The performance characteristics of significant components in the system are also investigated in term of exergetic efficiency. From the present field tests, the following results were obtained;

- (1) The thermal efficiency of SRCS with the mechanical feed pump is higher compared with the thermally driven pump. The reason comes from the lower value of pressure difference between supercritical (high) pressure and subcritical (low) pressure with the thermally driven pump. However, there is no electric consumption in the system with the thermally driven pump.
- (2) By using the thermally driven pump to the system, the exergetic efficiency was found higher compared with that of the mechanical feed pump: 20.28% and 11.47%, respectively.

- (3) The highest rate of exergy destruction rate is found in the evacuated solar collector for both system conditions. In case of SRCS with the mechanical feed pump, higher exergy destruction rate (89.99%) was obtained compared with the system with the thermally driven pump (76.28%). It is due to the heat loss in the evacuated solar collector.
- (4) Weather (seasonal) conditions have much effect on the exergetic efficiency by components in SRCS with the thermally driven pump, especially in turbine and high-temperature heat exchanger. In the winter season, the turbine gives highest exergetic efficiency, whereas the high-temperature heat exchanger gives the lowest exergetic efficiency, and vice versa in the summer season.

It can be concluded in term of energy and exergy analysis that the thermally driven pump improves the system to have higher performance characteristics. However, it is further suggested that the optimization in designing by components is required to enhance the highest performance in seasonal operations.

Nomenclature

A	solar collective area (m^2)
\dot{E}	exergy rate (kW)
h	specific enthalpy (kJ/kg)
I	solar irradiation (W/m^2)
\dot{m}	mass flow rate (kg/s)
P	pressure (MPa)
\dot{Q}	heat transfer rate (kW)
s	specific entropy (kJ/kg·K)
T	temperature ($^{\circ}C$ or K)
W	power (kW)

Greek symbols

η	efficiency (%)
η_e	system exergetic efficiency (%)
η_{th}	thermal efficiency (%)
η_x	component exergetic efficiency (%)
η_{ni}	percentage of exergy destruction (%)
Π	exergy destruction rate (kW)

Subscripts

0	dead state
1 ~ 9	positions ① ~ ⑨ shown in Figure 1
CO ₂	carbon dioxide
fp	mechanical feed pump
HX1	high-temperature heat exchanger
HX2	low-temperature heat exchanger
in	input
s	evacuated solar collector
sr	solar radiation
t	turbine
tp	thermally driven pump

Funding

The authors received no direct funding for this research.

Author details

Chayadit Pumaneratkul¹

E-mail: eup3502@mail4.doshisha.ac.jp

Takashi Horino¹

E-mail: ctwb0520@mail4.doshisha.ac.jp

Haruhiko Yamasaki²

E-mail: hyamasaki@me.osakafu-u.ac.jp

Hiroshi Yamaguchi¹

E-mail: hyamaguc@mail.doshisha.ac.jp

¹ Energy Conversion Research Center, Department of Mechanical Engineering, Doshisha University, 1-3 Tatara Miyakodani, Kyotanabe, Kyoto Prefecture, 610-0321, Japan.

² Department of Mechanical Engineering, Osaka Prefecture University, Sakai, Osaka Prefecture, 599-8531, Japan.

Citation information

Cite this article as: Exergy analysis of development on supercritical CO₂ solar Rankine cycle system with thermally driven pump, Chayadit Pumaneratkul, Takashi Horino, Haruhiko Yamasaki & Hiroshi Yamaguchi, *Cogent Engineering* (2018), 5: 1475440.

References

- Chaichan, M. T., & Kazem, H. A. (2016). Experimental analysis of solar intensity on photovoltaic in hot and humid weather conditions. *International Journal of Scientific & Engineering Research*, 7(3), 91–96.
- Chen, Q., Wang, M., Pan, N., & Guo, Z.-Y. (2009). Optimization principles for convective heat transfer. *Energy*, 34(9), 1199–1206. doi:10.1016/j.energy.2009.04.034
- Dimitrov, R. S. (2016). The Paris agreement on climate change: Behind closed doors. *Global Environmental Politics*, 16(3), 1–11. doi:10.1162/GLEP_a_00361
- Grosu, L., Marin, A., Dobrovicescu, A., & Queiros-Conde, D. (2016). Exergy analysis of a solar combined cycle: Organic Rankine cycle and absorption cooling system. *International Journal of Energy and Environmental Engineering*, 7(4), 449–459. doi:10.1007/s40095-015-0168-y
- Guo, T., Wang, H., & Zhang, S. (2010). Comparative analysis of CO₂-based transcritical Rankine cycle and HFC245fa-based subcritical organic Rankine cycle using low-temperature geothermal source. *Science China Technological Sciences*, 53(6), 1638–1646. doi:10.1007/s11431-010-3123-4
- Hepbasli, A. (2008). A key review on exergetic analysis and assessment of renewable energy resources for a sustainable future. *Renewable and Sustainable Energy Reviews*, 12(3), 593–661. doi:10.1016/j.rser.2006.10.001
- Hu, Y., Naito, S., Kobayashi, N., & Hasatani, M. (2000). CO₂, NO_x and SO₂ emissions from the combustion of coal with high oxygen concentration gases. *Fuel*, 79(15), 1925–1932. doi:10.1016/S0016-2361(00)00047-8
- Kanoglu, M., Dincer, I., & Rosen, M. A. (2007). Understanding energy and exergy efficiencies for improved energy management in power plants. *Energy Policy*, 35(7), 3967–3978. doi:10.1016/j.enpol.2007.01.015
- Kuwahara, T., Niu, X. D., Yamaguchi, H., Iwamoto, Y., & Zhang, X. R. (2011). Performance study of supercritical CO₂-based solar Rankine cycle system with a novel-concept thermally driven pump. *Proceedings of the Institution of Mechanical Engineers, Part A: Journal of Power and Energy*, 225(4), 413–419. doi:10.1177/0957650910396420
- Mago, P. J., Srinivasan, K. K., Chamra, L. M., & Somayaji, C. (2008). An examination of exergy destruction in organic Rankine cycles. *International Journal of Energy Research*, 32(10), 926–938. doi:10.1002/er.1406
- Petela, R. (2003). Exergy of undiluted thermal radiation. *Solar Energy*, 74(6), 469–488. doi:10.1016/S0038-092X(03)00226-3
- Pope, K., Dincer, I., & Naterer, G. F. (2010). Energy and exergy efficiency comparison of horizontal and vertical axis wind turbines. *Renewable Energy*, 35(9), 2102–2113. doi:10.1016/j.renene.2010.02.013
- PROPATH Group. (1997). *PROPATH: A program package for thermophysical properties, version 10.2*. Japan: Kyushu University.
- Ruppel, W., & Wurfel, P. (1980). Upper limit for the conversion of solar energy. *IEEE Transactions on Electron Devices*, 27(4), 877–882. doi:10.1109/T-ED.1980.19950
- Spayde, E., Mago, P. J., & Cho, H. (2017). Performance evaluation of a solar-powered regenerative organic Rankine cycle in different climate conditions. *Energies*, 10(1), 94. doi:10.3390/en10010094
- Suzuki, A. (1988). General theory of exergy-balance analysis and application to solar collectors. *Energy*, 13(2), 153–160. doi:10.1016/0360-5442(88)90040-0
- Tsatsaronis, G., & Czesla, F. (2004). *Exergy and thermodynamic analysis* (pp. 34–45). Oxford: Eolss Publishers.
- Wagner, W., & Pruß, A. (2002). The IAPWS formulation 1995 for the thermodynamic properties of ordinary water substance for general and scientific use. *Journal of Physical and Chemical Reference Data*, 31(2), 387–535. doi:10.1063/1.1461829
- Yamaguchi, H., Zhang, X.-R., Niu, X.-D., & Hashitani, N. (2013). A novel thermally driven pump and its test in a supercritical CO₂ loop system. *International Journal of Energy Research*, 37(11), 1331–1338. doi:10.1002/er.2934
- Zhang, X.-R., Yamaguchi, H., Fujima, K., Enomoto, M., & Sawada, N. (2005). A feasibility study of CO₂-based Rankine cycle powered by solar energy. *JSME International Journal Series B Fluids and Thermal Engineering*, 48(3), 540–547. doi:10.1299/jsmeb.48.540
- Zhang, X.-R., Yamaguchi, H., & Uneno, D. (2007). Experimental study on the performance of solar Rankine system using supercritical CO₂. *Renewable Energy*, 32(15), 2617–2628. doi:10.1016/j.renene.2007.01.003
- Zhang, X. R., Yamaguchi, H., Uneno, D., Fujima, K., Enomoto, M., & Sawada, N. (2006). Analysis of a novel solar energy-powered Rankine cycle for combined power and heat generation using supercritical carbon dioxide. *Renewable Energy*, 31(12), 1839–1854. doi:10.1016/j.renene.2005.09.024



© 2018 The Author(s). This open access article is distributed under a Creative Commons Attribution (CC-BY) 4.0 license.

You are free to:

Share — copy and redistribute the material in any medium or format.

Adapt — remix, transform, and build upon the material for any purpose, even commercially.

The licensor cannot revoke these freedoms as long as you follow the license terms.

Under the following terms:

Attribution — You must give appropriate credit, provide a link to the license, and indicate if changes were made.

You may do so in any reasonable manner, but not in any way that suggests the licensor endorses you or your use.

No additional restrictions

You may not apply legal terms or technological measures that legally restrict others from doing anything the license permits.

Cogent Engineering (ISSN: 2331-1916) is published by Cogent OA, part of Taylor & Francis Group.

Publishing with Cogent OA ensures:

- Immediate, universal access to your article on publication
- High visibility and discoverability via the Cogent OA website as well as Taylor & Francis Online
- Download and citation statistics for your article
- Rapid online publication
- Input from, and dialog with, expert editors and editorial boards
- Retention of full copyright of your article
- Guaranteed legacy preservation of your article
- Discounts and waivers for authors in developing regions

Submit your manuscript to a Cogent OA journal at www.CogentOA.com

